Journal of Applied Polymer Science

The Morphology and Degradation Behavior of Electrospun Poly(3-hydroxybutyrate)/Magnetite and Poly(3-hydroxybutyrate-*co*-3-hydroxyvalerate)/Magnetite Composites

Mao-Hsun Ho,[1] Si-Yu Li,[2] Chun-Yu Ciou,[1] Tzong-Ming Wu[1]

[1]Department of Materials Science and Engineering, National Chung Hsing University, Taichung, Taiwan

[2]Department of Chemical Engineering, National Chung Hsing University, Taichung, Taiwan

Correspondence to: T.-M. Wu (E-mail: tmwu@dragon.nchu.edu.tw)

ABSTRACT: Electrospinning of biodegradable poly(3-hydroxybutyrate) (PHB)/magnetite and poly(3-hydroxybutyrate-*co*-3-hydroxyvalerate) (PHBV)/magnetite composites in 2,2,2-trifluoroethanol (TFE) and chloroform are investigated to develop nonwoven nanofibrous structure. Ultrafine PHB/magnetite fibers are obtained and the resulting fiber diameters are in the range of 690–710 nm and 8.0–8.4 μm for the polymer dissolved in TFE and chloroform. The surface of PHB composites fiber fabricated in chloroform contains porous structures, which are not observed for the sample of PHB composites fiber dissolved in TFE. The fiber diameters for PHBV5/magnetite composites are in the range of 500–540 nm and 2.3–2.5 μm, depending on the use of TFE and chloroform. The average diameters of PHBV5/magnetite composite fibers are smaller than those of PHB/magnetite composites fiber. All electrospun PHB/magnetite and composite fibers are superparamagnetic. The degradation behaviors of PHB/magnetite and PHBV5/magnetite composite fibers were investigated using *Caldimonas manganoxidans*. For the fabricated composite fibers, it is found that the degradation rate increased with the increasing loading of magnetite nanoparticles. © 2014 Wiley Periodicals, Inc. J. Appl. Polym. Sci. **2014**, *131*, 41070.

KEYWORDS: biodegradable; composites; degradation

Received 19 February 2014; accepted 28 May 2014
DOI: 10.1002/app.41070

INTRODUCTION

In the present era of reducing petrochemical feedstock and increasing environmental awareness, biocompatible, and biodegradable polymers are widely used as attractive substitutes for conventional petroleum-derived plastics. The most widely used biodegradable polymers, such as poly(3-hydroxybutyrate) (PHB), poly(lactic acid), poly(ε-caprolactone), and poly(butylenes succinate), have attracted more attention because of its renewable resources, biodegradability, and outstanding physical and mechanical properties. As a result, they have potential uses in packages and biomedical implants.[1–3] Among these biodegradable polymers, PHB belongs to a family of poly(hydroxyalkanoates) (PHAs), which can be synthesized by many bacteria as a reserve energy source.[4,5] Moreover, PHB is a thermoplastic polymer containing physical and mechanical properties close to those of isotactic polypropylene, which can be extensively processed using conventional processing equipments. To enhance the processing and mechanical properties, the poly(3-hydroxybutyrate-*co*-3-hydroxyvalerate) (PHBV) with various ratios of 3-hydroxyvalerate (HV) was introduced.[6,7] The alternative approach to enhance the mechanical properties of PHB materials is to blend inorganic nanoparticle with PHB.[8,9] Nevertheless, the preparation and degradation behaviors of biodegradable polymer/inorganic nanoparticle composites are seldom mentioned among these reports.

Nanometer sized iron oxide in the crystalline form of magnetite (Fe_3O_4) containing ferromagnetic and supermagnetic properties has received considerable attention due to its numerous applications in various fields such as magnetic recording media, giant magnetoresistive sensors, and photonic crystals.[10–15] Magnetic properties of nanoparticles are associated with finite-size and surface effects. Recently, the preparation of relatively stabilized and uniform Fe_3O_4 using oleic acid as a surfactant was reported.[12–14] Because the oleic acid has higher affinity to the surface of superfine Fe_3O_4 as compared to other surfactants, it can form a waterproof shell around the Fe_3O_4 nanoparticles.[15] Therefore, obtaining well-distributed Fe_3O_4 in polymer matrix remains a challenging task.

Fabrication of polymer nanofibers can provide a high surface area for a given mass or volume. Electrospinning process involved the application of a strong electrostatic field between a

Additional Supporting Information may be found in the online version of this article.

capillary, connected to a tank containing a polymer solution, and a ground collector is a simple and quick method for generating polymer nanofibers. The choice of solvent has tremendous effects on the electrospinning process. Different solvents provide different viscosity, surface tension, conductivity, and volatility. The combination of aforementioned properties yields various rheological and electrostatic behaviors that subsequently lead to fibers electrospun in different diameters, alignments, and structures.[16] It is generally known that increasing viscosity of the polymer solution leads fibers in larger diameters. Decreasing the surface tension of the polymer solution effectively preventing the formation of the beads.[17] It has been shown that the fibers can be orderly electrospun by choosing a suitable solvent with the appropriate dielectric properties.[18] The solvent volatility has been related to the porous structure of electrospun fibers. A rapid phase separation resulting from a high solvent evaporation rate can be induced upon the right combination of polymer/solvent systems and therefore generates porous structures.[19,20] Solvent effects on jet evolution during the electrospinning process have been detailed discussed previously.[21,22] The effect of ions in the solvent has also been discussed. The addition of 1 wt % KH_2PO_4, NaH_2PO_4, or NaCl, which increased the charge density of the polymer solution, prohibited the formation of beads-on-string structure with relatively smaller diameters.[23] One promising application of PHB/Fe_3O_4 materials in biomedical engineering is to arguably enhance bone tissue regeneration by stimulated static magnetic fields provided by superparamagnetic Fe_3O_4 nanoparticles.[8,24]

In this study, we propose an approach to fabricated a nonwoven biodegradable PHB/magnetite and PHBV/magnetite composite fibers using electrospinning process where 2,2,2-trifluoroethanol (TFE) and chloroform are individually used as solvents. The incorporation of magnetite nanoparticles into polymer matrix could slightly increase the viscosity and dielectric properties of composites. The structure, morphology, and magnetic properties of the PHB/magnetite and PHBV5/magnetite nanocomposites were characterized using FESEM and SQUID. The degradation behavior of composite fiber were investigated using *Caldimonas manganoxidans* (ATCC BAA-369=JCM 10698=IFO 16448=BCRC17858), which is a gram-negative, aerobic, rod-shaped, and thermophilic bacterium. It was isolated from a hot spring in Matsue, Japan, where the optimum temperature and pH for growth were 45–50°C and 7–8, respectively.[25] It is known for oxidizing manganese and degrading PHB. It has been shown that the PHB depolymerase is stable up to 65°C and has a maximum reaction rate at 70°C.[26]

EXPERIMENTAL

Materials

Chloroform and TFE purchased from Mallinckrodt Baker and Fluka were used without purification. Iron (III) acetylacetonate, oleic acid, and oleylamine were supplied from Acros, Showa and Sigma-Aldrich. *Caldimonas manganoxidans* (ATCC BAA-369=JCM 10698=IFO 16448=BCRC17858) was purchased from the Bioresource Collection and Research Center (BCRC), Hsinchu, Taiwan. PHB with number-average molecular weight (M_n) of 2.9×10^5 and PHBV (PHBV5 with PHV content of 5%) with M_n of 1.4×10^5 purchased from Sigma-Aldrich Chemical were purified by mixing PHB and PHBV5 in chloroform solution and then refluxed at 60°C for 4 h. The solution was precipitated by adding *n*-hexane into the PHB/chloroform and PHBV5/chloroform solution. The purified PHB and PHBV5 were filtrated and then vacuum dried at 40°C for 24 h. The monodispersed 6 nm magnetite nanoparticles were prepared using the thermal decomposition of a mixture of Iron (III) acetylacetonate, oleic acid, 1,2-hexadecanediol oleylamine, and phenyl ether, which were added into a three-necked bottle and purged with N_2 to inhibit the effect of oxygen. The solution was heated to 200°C for 2 h and further heated to reflux at 300°C for 60 min. Then the mixture was precipitated with ethanol, centrifuged to remove the solvent, and redispersed into hexane.

Preparation of PHB/Magnetite and PHBV5/Magnetite Electrospun Fibers

To fabricate the uniform distribution of magnetite in polymer matrix, various weight ratios of magnetite were dispersed in chloroform and TFE. The solution was ultrasonicated over 6 h. The PHB and PHBV5 were also dissolved in chloroform and TFE. Various concentrations of PHB/magnetite and PHBV5/magnetite solution were prepared by the mixing PHB/PHBV5 and 6 nm magnetite nanoparticles in chloroform and TFE. The solution of mixture was ultrasonicated over 12 h. The polymer solution was then stored in a 2.5 mL syringe with a 22 gauge needle, which was mounted on an infusion pump. The spinning direction was from the left to the right. A voltage of 12 kV was applied to the needle by a high voltage power supply; this value was chosen because the fibers showed good homogeneity at this voltage. A flat piece of aluminum foil, placed 20 cm away the capillary tip, was used to collect the electrospun fibers.

Characterization of PHB/Magnetite and PHBV5/Magnetite Electrospun Fibers

Field-emission scanning electron microscopy (FESEM) conducted at 3 kV using a JEOL JSM-6700F field-emission instrument was used to characterize the morphology of the PHB/magnetite and PHBV5/magnetite composite fibers. A Superconductor Quantum Interference Device (SQUID) was used at room temperature to study the magnetic properties. The crystallization behavior of the PHB/magnetite and PHBV5/magnetite composite fibers was investigated by differential scanning calorimetry (DSC). The calorimetric analysis was carried out on a PYRIS Diamond DSC. All specimens weighted about 3 mg were heated from 10 to 190°C at a rate of 100°C/min. The enthalpy of fusion (ΔH_m) of PHB/magnetite and PHBV5/magnetite composite were recorded. According to the enthalpy of fusion, the relative crystallinity (X_c) of composite fibers could be determined using $X_c(\%) = \frac{\Delta H_m}{(1-\phi)\Delta H_m^0} \times 100\%$. The value of ΔH_m^0, the enthalpy of fusion of 100% crystallize PHB polymer, is 146 J/g and φ is the weight fraction of the magnetite in the nanocomposites.[27] Because the content of PHV in PHBV5 is low, the value of ΔH_m^0 can be assumed to be the same as that of pure PHB. The *in vitro* degradation behaviors of sample were operated using *Caldimonas manganoxidans*. To conduct the microbial degradation of composite fibers, *Caldimonas*

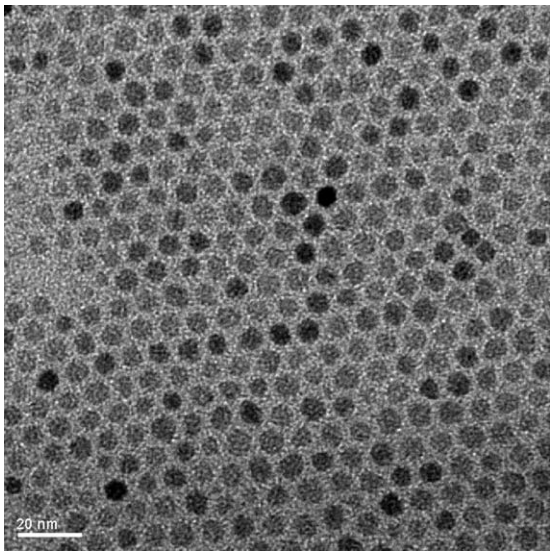

Figure 1. HRTEM images of monodispersed 6 nm magnetite nanoparticles.

manganoxidans was firstly activated in PY medium (10 g/L, polypeptone; 2 g/L, yeast extract; 1 g/L $MgSO_4 \cdot 7H_2O$) at 45°C and 200 rpm for 2 days. 1% inoculum was transferred to a fresh PY medium and 3 mL of this fresh microbial solution was distributed to each cell of a 12-well plate to submerge the composite fiber sample in it. The 12-cell plate was then placed in a shaking incubator at 55°C, 100 rpm, and 50% relative humidity (RH). All composite fiber samples were sterilized by UV radiation for 15 min before the microbial degradation test. The biodegradability of electrospun fibers was quantified by measuring the percent of weight residue of electrospun fibers during the microbial degradation. The measurement of the residual weight of electrospun fibers was done by firstly removing fiber samples from the 12-cell plate during the microbial degradation test. The fiber samples were cleaned with DI water and dried at 40°C for 24 h before weighing. After weighing the weight, the electrospun fibers were sterilized by UV radiation for another 15 min and placed back to the 12-cell plate for the continuation of the microbial degradation test.

RESULTS AND DISCUSSION

Preparation of PHB/Magnetite and PHBV5/Magnetite Electrospun Fibers

Figure 1 reveals the HRTEM images of monodispersed 6 nm Fe_3O_4 synthesized using the thermal decomposition of iron acetylacetonate with oleic acid in the presence of high boiling point solvents. From this result, the average diameter of Fe_3O_4 particle size is about 6 nm and its distribution is extremely uniform. The processing parameters of electrospinning consist of the polymer concentration, deposition distance, flow rate, and applied field strength. The minimum polymer concentration to form the continuous fiber at a flow rate of 0.2 mL/h is about 5 wt % PHB and PHBV5 dissolved in TFE with the deposition distances of 20 cm and applied field strength of 12 kV. The fiber structure of PHB and PHBV5 was affected by changing the parameters of polymer concentration and flow rate. But we can not obtain the continuous fiber for PHB/chloroform and PHBV5/chloroform solution by using the same parameters of electrospinning. Therefore, we examine the diameter variations of electrospun fiber with different flow rates, while the concentration of PHB and PHBV5 in TFE and chloroform was kept constant at 10 wt % with the deposition distances of 20 cm and applied field strengths of 12 kV. The minimum flow rate to form the continuous fiber is about 4 mL/h for PHB and PHBV5 dissolved in chloroform. To better understand the effect of solvent on the microstructure of electrospun fiber, morphological analysis was performed using field-emission scanning electron microscopy (FESEM) to investigate the surface and fiber diameter of the composite fibers. Figure 2 shows a series of FESEM micrographs of PHB/magnetite composite fibers prepared using TFE and chloroform. In both case, the continuous and bead-free fiber could be fabricated and collected continuously for long times. As it can be seen, the fibers were obtained with quite uniform size distributions. With increasing flow rate, the fiber diameter obtained for each sample with the same experimental parameters could be moderately increased. The average fiber diameters were in the range of 690–710 nm and 8.0–8.4 μm for the polymer dissolved in TFE and chloroform. It is also noted that the surface of PHB composites fiber obtained using chloroform contains porous structure, which did not observe for the sample of PHB composites fiber with TFE. The average pore size is in the order of 1 μm. This result is probably because of the rapid phase separation of PHB/chloroform system during electrospinning process. The solvent rich area could transform into pore during the evaporation of solvent. Figure 3 shows the FESEM images of PHBV5/magnetite fabricated using TFE and chloroform. The results are similar to those observed for PHB/magnetite composites fiber. The fiber diameters were in the range of 500–540 nm and 2.3–2.5 μm, depending on the use of solvent. The average diameters of PHBV5/magnetite composite fibers were smaller than those of PHB/magnetite composites fiber. This result might be due to the addition of more flexible HV unit into the rigid PHB homopolymer chain induced the formation of small Taylor cone during electrospinning process. Figure 4 reveals the backscatter electron imaging (BEI) mode of the FESEM for the composites fiber with 5 wt % loading of magnetites. The bright spot of FESEM images present the possible distribution of magnetite. From this result, the distribution of magnetite is quite uniform within polymer matrix.

Characterization of PHB/Magnetite and PHBV5/Magnetite Electrospun Fibers

The crystallization behavior of PHB/magnetite and PHBV5/magnetite materials was performed using DSC. The data of thermal properties for PHB/magnetite and PHBV5/magnetite composites are summarized in Table I. Figure 5 illustrates the DSC heating scans of PHB/magnetite and PHBV5/magnetite composite fibers fabricated using TFE and chloroform. One melting peak was observed on the melting curve of all PHB/magnetite and PHBV5/magnetite system. The melting peaks of composite were almost the same compared to that of pure polymer matrix. The enthalpy of fusion (ΔH_m) and relative

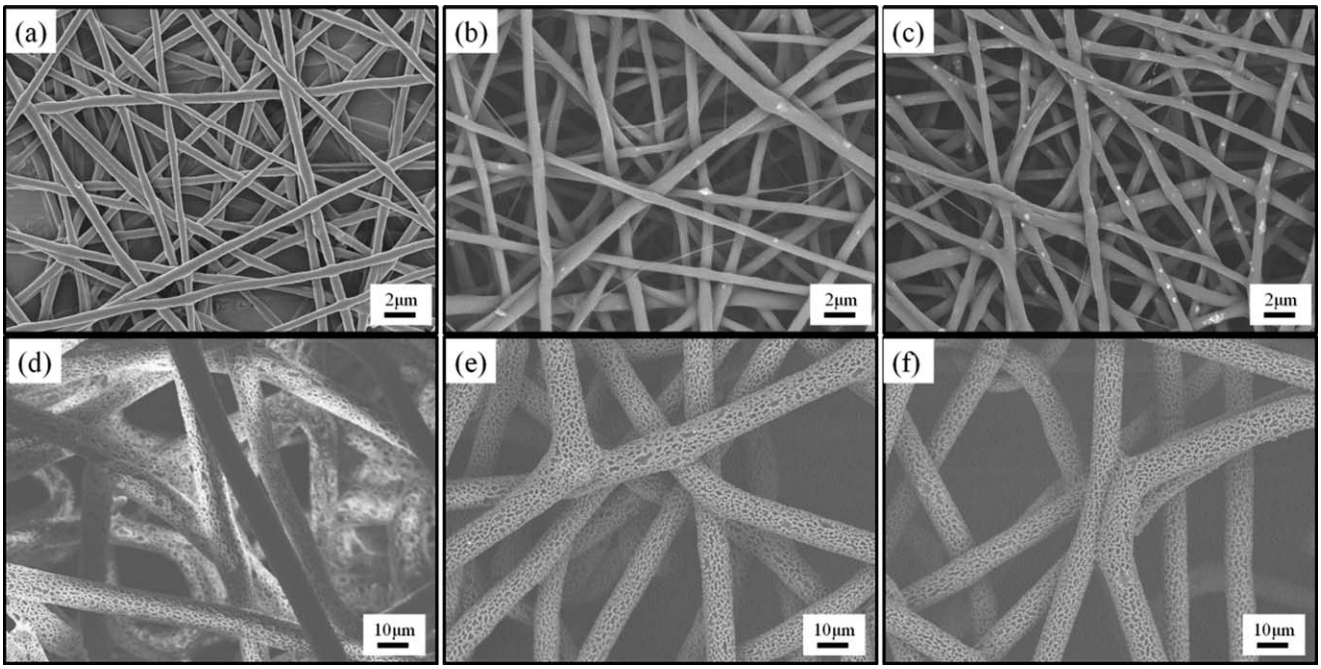

Figure 2. FESEM images of (a) PHB, (b) 1 wt % PHB/magnetite, and (c) 5 wt % PHB/magnetite dissolved in TFE. FESEM images of (d) PHB, (e) 1 wt % PHB/magnetite, and (f) 5 wt % PHB/magnetite dissolved in chloroform.

crystallinity (X_c) of PHB/magnetite and PHBV5/magnetite composite recorded in Table I reveal that the incorporation of magnetite particle would decrease the crystallinity of PHB and PHBV5. This result might be contributed to the restriction of polymer chain arrangement with the presence of magnetite.

The magnetic properties of PHB/magnetite and PHBV5/magnetite composite fibers were measured using VSM system. Typical magnetization curves of 1 and 5 wt % PHB/magnetite composite fibers dissolved in TFE with the applied magnetic field at room temperature are shown in Figure 6. Because the PHB and PHBV5 are not magnetic, the magnetic properties of the fabricated composite fibers are strongly dependent on the contents of monodispersed 6 nm Fe_3O_4 nanoparticles. The magnetic properties of nanocomposites indicated supermagnetism with

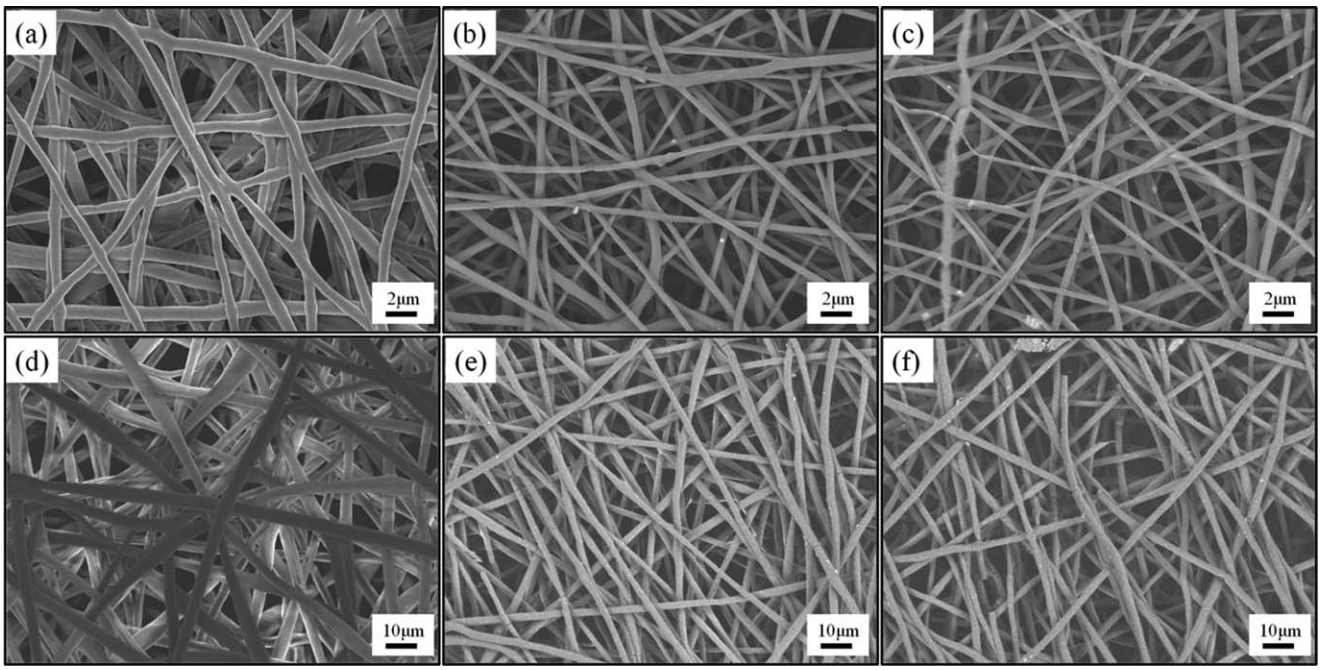

Figure 3. FESEM images of (a) PHBV5, (b) 1 wt % PHBV5/magnetite, and (c) 5 wt % PHBV5/magnetite dissolved in TFE. FESEM images of (d) PHBV5, (e) 1 wt % PHBV5/magnetite, and (f) 5 wt % PHBV5/magnetite dissolved in chloroform.

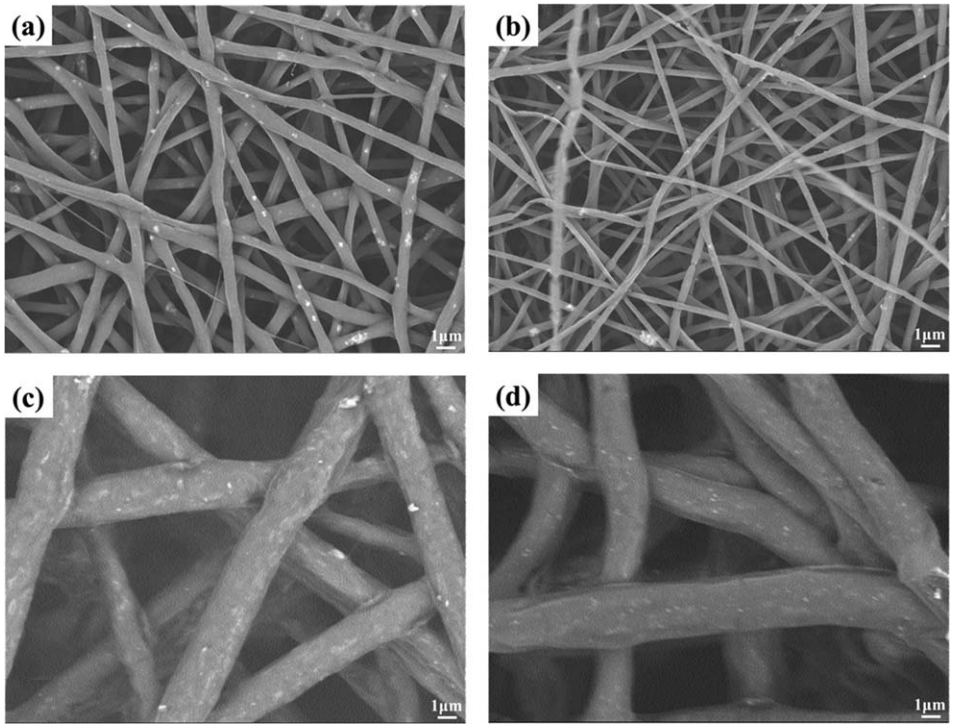

Figure 4. The backscatter electron imaging (BEI) mode of the FESEM for the (a) 5 wt % PHB/magnetite dissolved in TFE, (b) 5 wt % PHBV5/magnetite dissolved in TFE, (c) 5 wt % PHB/magnetite dissolved in chloroform, and (d) 5 wt % PHBV5/magnetite dissolved in chloroform.

saturation magnetization (M_s) of 1 wt % PHB/magnetite composite was 0.61 emu/g. Increasing magnetite content from 1 to 5 wt %, the value of M_s raised to 2.47 emu/g. The data of magnetic properties for PHB/magnetite and PHBV5/magnetite composites prepared using TFE and chloroform are summarized in Table I. All composite fibers contain supermagnetic properties.

Table I. Thermal and Magnetic Properties of PHBV/Magnetite Composite Fibers Fabricated Using TFE and Cholorform

Sample	ΔH_m (J/g)	X_c[a] (%)	M_s (emu/g)
PHB (TFE)	84.2	57.7	-
1 wt % PHB/magnetite (TFE)	78.4	54.2	0.61
5 wt % PHB/magnetite(TFE)	72.9	46.5	2.47
PHBV5 (TFE)	64.5	44.2	-
1 wt % PHBV5/magnetite (TFE)	59.7	41.3	0.43
5 wt % PHBV5/magnetite (TFE)	55.4	39.9	2.22
PHB (chloroform)	83.1	56.9	-
1 wt % PHB/magnetite (chloroform)	76.7	53.1	0.42
5 wt % PHB/magnetite (chloroform)	66.4	47.9	2.18
PHBV5 (chloroform)	65.7	45	-
1 wt % PHBV5/magnetite (chloroform)	59.2	40.1	0.57
5 wt % PHBV5/magnetite (chloroform)	56.2	40.5	2.51

[a] X_c is the obtained by the following equation using ΔH_m^0=146 J/g and φ is the weight fraction of the magnetite in the nanocomposites.
$X_c(\%)=\frac{\Delta H_m}{(1-\phi)\Delta H_m^0}\times 100\%$

The increase of saturation magnetization is attributed to the amount of monodispersed Fe_3O_4 nanoparticles in composites. According to our experimental data, the increasing the amounts of 6 nm monodispersed Fe_3O_4 nanoparticles may be resulted in the increasing saturation magnetization.

Biodegradability of PHB/Magnetite and PHBV5/Magnetite Electrospun Fibers

The biodegradability of PHB/magnetite and PHBV5/magnetite composite fibers electrospun with TFE or chloroform was investigated using *Caldimonas manganoxidans*. During the biodegradability test, each composite fiber together with *Caldimonas manganoxidans* seeds was incubated in the fresh medium. Figures 7 and 8 show the weight residue of PHB/magnetite and PHBV5/magnetite electrospun composite fibers dissolved in TFE or chloroform. While PHB and PHBV5 electrospun fibers with TFE or chloroform can be readily degraded by *Caldimonas manganoxidans*, the addition of Fe_3O_4 enhanced the biodegradability of composite fibers. It has been shown previously that Fe^{2+} severely inhibited the activity of PHB depolymerase[28] while Fe^{3+} has no effect on the activity of PHB depolymerase.[29] The enhanced biodegradability with the addition of Fe_3O_4 is presumably attributed to the decrease of the crystallinity rather than the chemical interaction of Fe_3O_4 and enzymes. Meanwhile, PHBV5 fibers showed a faster degradation rate than that of PHB fibers. It has been shown before that the biodegradability highly depends on the crystallinity and elastic modulus. The biodegradability increases as the crystallinity of the materials decreases.[30] Since PHBV5 has a lower degree of crystallinity, it is reasonable to see that PHBV5 fibers showed a

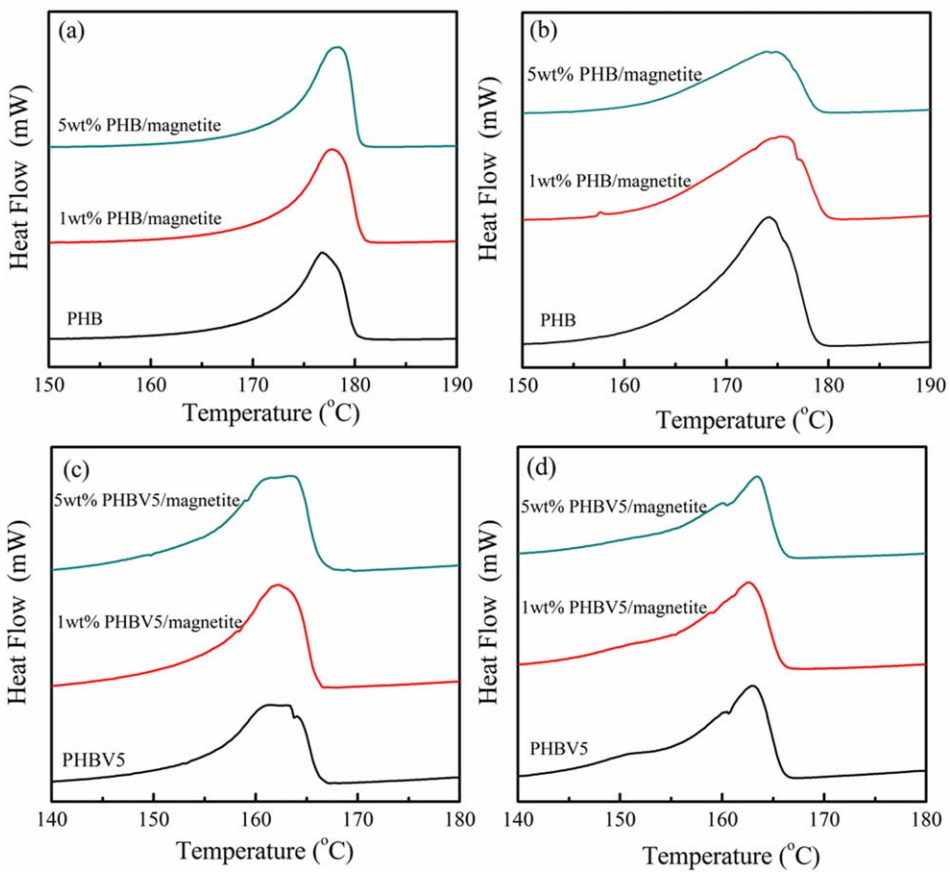

Figure 5. DSC heating scans of PHB, 1 wt % PHB/magnetite and 5 wt % PHB/magnetite dissolved in (a) TFE and (b) chloroform. DSC heating scans of PHBV5, 1 wt % PHBV5/magnetite and 5 wt % PHBV5/magnetite dissolved in (c) TFE and (d) chloroform. [Color figure can be viewed in the online issue, which is available at wileyonlinelibrary.com.]

faster degradation rate than that of PHB fibers. Solvent effects on the biodegradability of electrospun fibers were also shown in Figures 6 and 7 where the fibers electrospun with chloroform provided a faster degradation rate as compared to the fibers electrospun with TFE. This can be attributed to the effect of surface morphology where lumpy surface structure was formed with chloroform (Figure 2). This lumpy surface facilitated the colonization of the bacterial culture and thus increased the biodegradation rate. It can be seen in Figure 8(b) that 1 wt % PHBV5/magnetite and 5 wt % PHBV5/magnetite composite fibers electrospun with chloroform conferred the fastest degradation rate among the tested materials. The 5 wt % PHBV5/magnetite fibers electrospun with chloroform lost more than 70% weight after 24 h of the microbial treatment and was nearly completely degraded at 36 h. Note that it was found that once the sample weight percentage was brought down below 10 %, a fiber sample became no longer an integrity but fragments. Therefore, it becomes tedious to handle the fiber samples and makes the measurement of residual fibers inaccurately. Therefore, it is concluded that when PHBV5 is used as the base fiber material, the addition of Fe_3O_4, and the use of chloroform are favored in terms of the biodegradability. Results discussed above were supported by SEM pictures as shown in Figures 9 and 10, where the fibers were taken for pictures after 0, 24, and 48 h treatment. It should be noted that there was no SEM picture of PHBV5 electrospun with chloroform at 48 h since the fibers was nearly completely degraded.

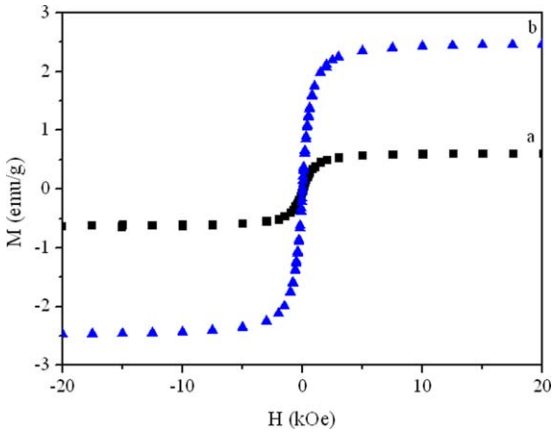

Figure 6. Magnetic properties of (a) 1 wt % PHB/magnetite and (b) 5 wt % PHB/magnetite dissolved in TFE. [Color figure can be viewed in the online issue, which is available at wileyonlinelibrary.com.]

The PHB depolymerase of *Caldimonas manganoxidans* has been purified and characterized previously.[31] It is an extracellular enzyme and the size of the mature protein is 46 kDa. The PHB

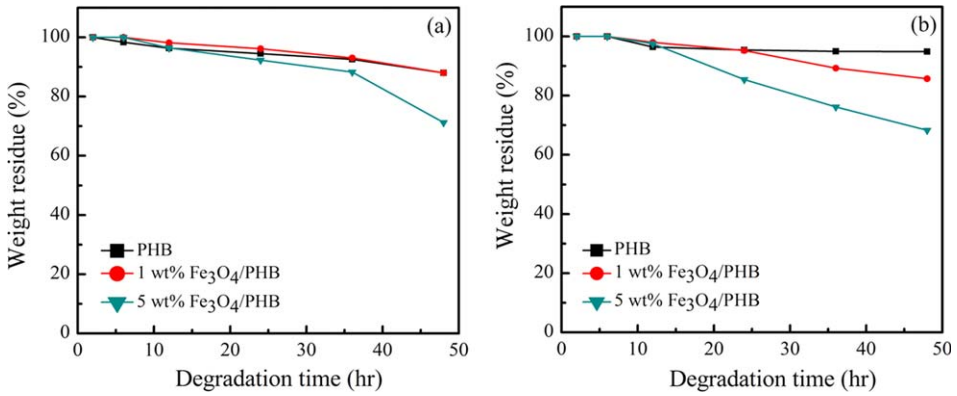

Figure 7. Weight residue of PHB, 1 wt % PHB/magnetite and 5 wt % PHB/magnetite dissolved in (a) TFE and (b) chloroform. [Color figure can be viewed in the online issue, which is available at wileyonlinelibrary.com.]

depolymerase is suggested to be classified as Type II. It contains three distinct domains. The first is the catalytic domain where the lipase box, G-L-S-S-G, is found herein. The second and third domains are fibronectin Type III and PHB-binding domains accordingly. Previous studies of the PHB depolymerase of *Caldimonas manganoxidans* has been limited to the enzymatic level. To the best of the authors' knowledge, this is the first report to demonstrate the efficacy of the microbial degradation of PHB and PHBV5 materials by total whole cell of *Caldimonas manganoxidans*. It should be noted that a fungus *Penicillium pinophilum* was used for testing the biodegradability of the composite fibers.[32] No degradation was observed after a 28 day treatment. By SEM pictures, it is concluded that the mycelia generated by *Penicillium pinophilum* covered the surface of PHB or PHBV5 composite fibers and thus hindered the accessibility of PHB depolymerase (see Supporting Information). Besides, the microbial degradation of composite fibers by total whole cell of *Caldimonas manganoxidans* was not observed when glucose was presence in the medium. This result supports a previous study that the expression of *Caldimonas manganoxidans* PHB depolymerases down-regulated by the presence of assimilable carbon sources and is up-regulated by the presence of 3-hydroxybutyrate.[28] The other possibility is that the magnetite incorporated in the electrospun fibers might serve as a growth factor that stimulated the bacteria growth and thus more PHB depolymerases were being made and secreted.[33]

CONCLUSIONS

Ultrafine PHBV5/magnetite composite fibers were successfully fabricated using electrospinning process. The resulting fiber diameters of PHB/magnetite were in the range of 690–710 nm and 8.0–8.4 μm for the polymer dissolved in TFE and chloroform. The surface of PHB composites fiber fabricated in chloroform contained porous structure, which did not observe for the sample of PHB composites fiber dissolved in TFE. The average pore size was in the order of 1 μm. This result is probably due to the rapid phase separation of PHB/chloroform system during electrospinning process. The fiber diameters for PHBV5/magnetite composites were in the range of 500–540 nm and 2.3–2.5 μm, depending on the use of solvent of TFE and chloroform. The average diameters of PHBV5/magnetite composite fibers were smaller than those of PHB/magnetite composites fiber. This result might be due to the addition of more flexible HV unit into the rigid PHB homopolymer chain induced the formation of small

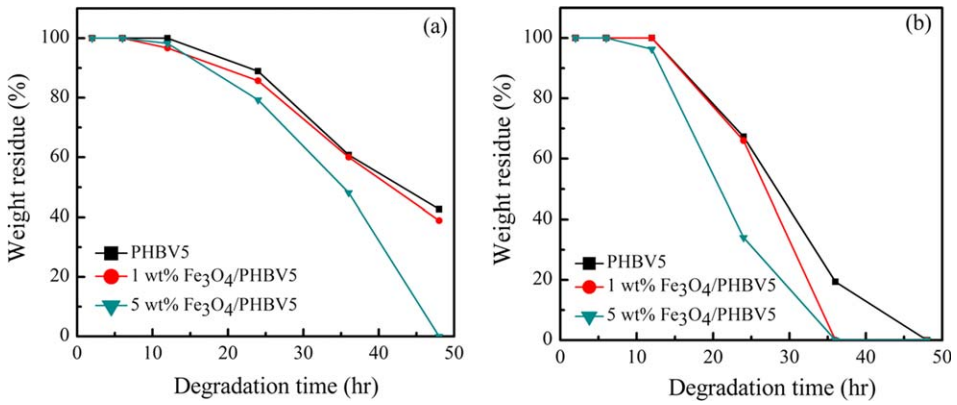

Figure 8. Weight residue of PHBV5, 1 wt % PHBV5/magnetite and 5 wt % PHBV5/magnetite dissolved in (a) TFE and (b) chloroform. [Color figure can be viewed in the online issue, which is available at wileyonlinelibrary.com.]

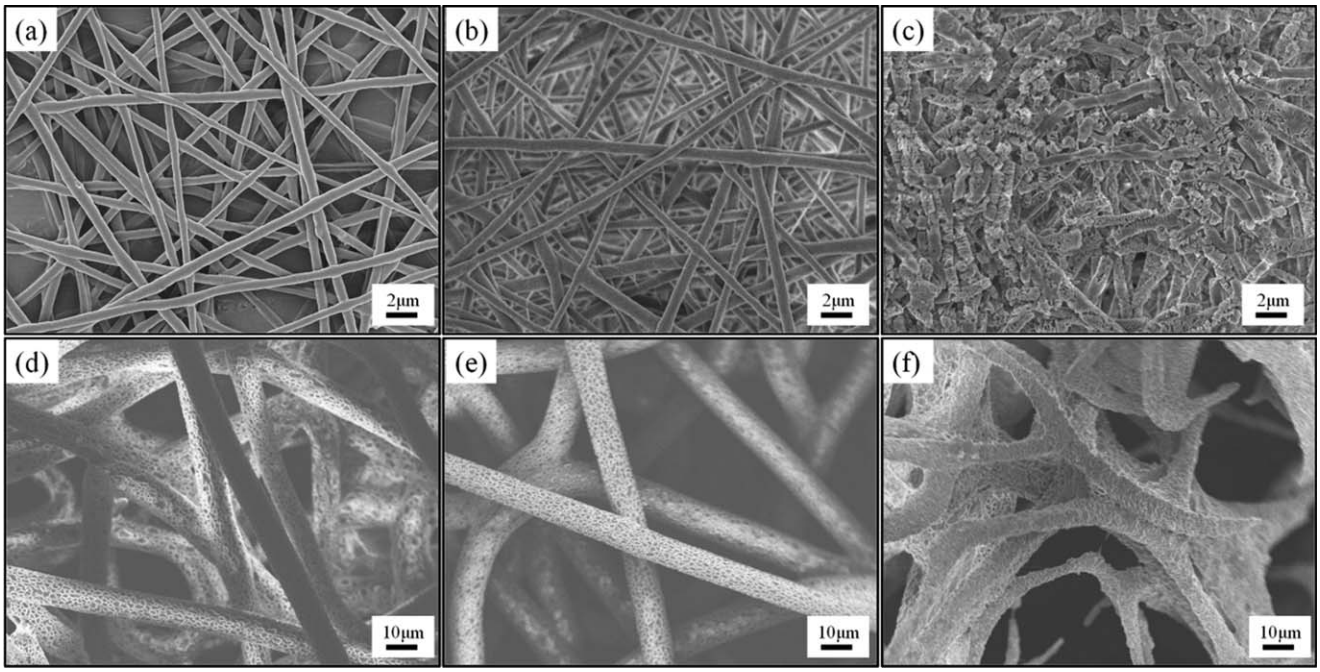

Figure 9. FESEM images of PHB/TFE after biodegradation test for (b) 24 h and (c) 48 h. FESEM images of PHB/chloroform after biodegradation test for (e) 24 h and (f) 48 h. For comparison, FESEM images of (a) PHB/TFE and (d) PHB/chloroform before degradation test were also shown in this figure.

Taylor cone during electrospinning process. The magnetic properties of PHBV5/magnetite composite fibers were superparamagnetic. The degradation behaviors of PHBV5/magnetite composite fibers were investigated using *Caldimonas manganoxidans*. The degradation rate of PHBV5 composite fibers was fast as compared to that of PHB/magnetite specimens. For PHBV5/magnetite composite fibers, the degradation rate increased with the increasing loading of magnetite nanoparticles. This result can be attributed to the incorporation of more magnetite nanoparticles into PHBV5 matrix, which might serve as a growth factor to stimulate the bacteria growth and then increase the degradation rate for PHBV5/magnetite composite fibers.

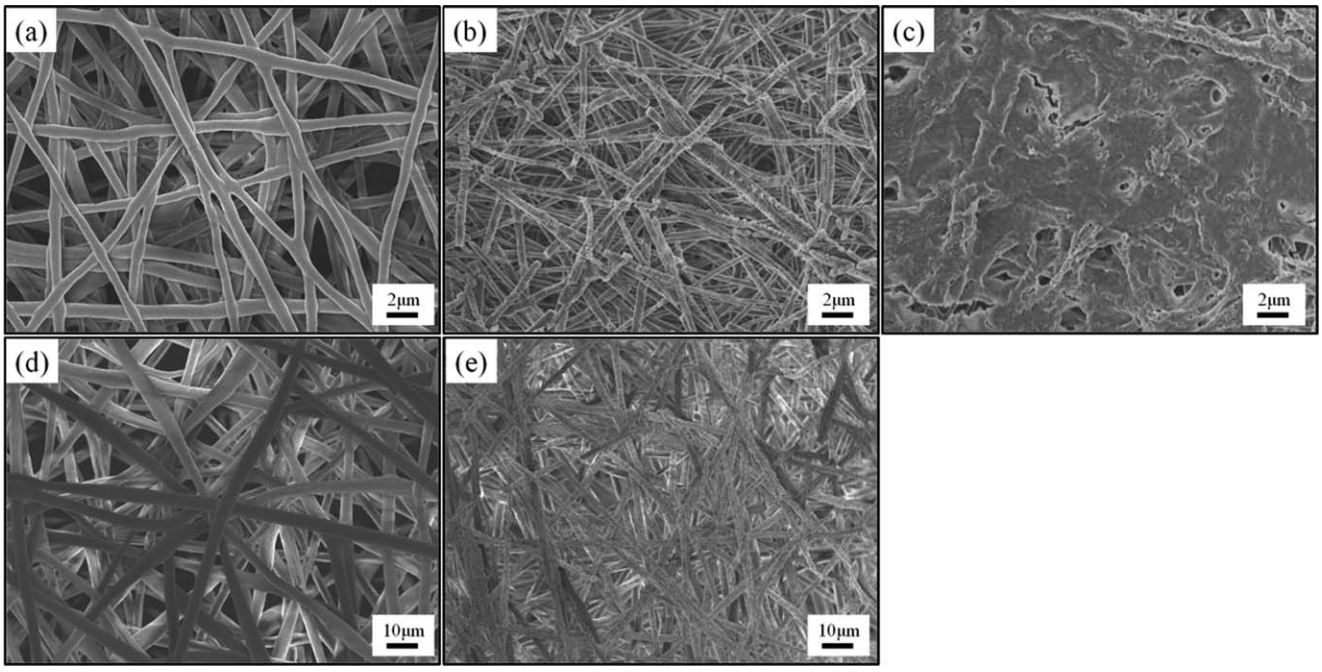

Figure 10. FESEM images of PHBV5/TFE after biodegradation test for (b) 24 h and (c) 48 h. FESEM images of PHBV5/chloroform after biodegradation test for (e) 24 h. For comparison, FESEM images of (a) PHBV5/TFE and (d) PHBV5/chloroform before degradation test were also shown in this figure.

ACKNOWLEDGMENTS

The financial support provided by National Science Council through the project NSC99-2212-E-005-012-MY3 is greatly appreciated.

REFERENCES

1. Ikada, Y.; Tsuji, H. *Macromol. Rapid Commun.* **2000**, *21*, 117.
2. Sinha Ray, S.; Bousmina, M. *Prog. Mater. Sci.* **2005**, *50*, 962.
3. Leung, V.; Ko, F. *Polym. Adv. Technol.* **2011**, *22*, 350.
4. Juzwa, M.; Jedliñski, Z., *Macromolecules* **2006**, *39*, 4627.
5. McChalicher, C. W. J.; Srienc, F.; Rouse, D. P. *AlChE J.* **2010**, *56*, 1616.
6. Ten, E.; Jiang, L.; Wolcott, M. P. *Carbohydr. Polym.* **2012**, *90*, 541.
7. Sankar, D.; Chennazhi, K. P.; Nair, S. V.; Jayakumar, R. *Carbohydr. Polym.* **2012**, *90*, 725.
8. Rezwan, K.; Chen, Q. Z.; Blaker, J. J.; Boccaccini, A. R., *Biomaterials* **2006**, *27*, 3413.
9. Kawasumi, M.; Hasegawa, N.; Kato, M.; Usuki, A.; Okada, A. *Macromolecules* **1997**, *30*, 6333.
10. Raj, K.; Moskowitz, B.; Casciari, R. *J. Magn. Magn. Mater.* **1995**, *149*, 174.
11. Xu, X.; Friedman, G.; Humfeld, K. D.; Majetich, S. A.; Asher, S. A. *Adv. Mater.* **2001**, *13*, 1681.
12. Sun, S.; Zeng, H. *J. Am. Chem. Soc.* **2002**, *124*, 8204.
13. Jana, N. R.; Chen, Y.; Peng, X. *Chem. Mater.* **2004**, *16*, 3931.
14. Yu, W. W.; Falkner, J. C.; Yavuz, C. T.; Colvin, V. L. *Chem. Commun.* **2004**, 2306.
15. Lin, C.-R.; Chiang, R.-K.; Wang, J.-S.; Sung, T.-W. *J. Appl. Phys.* **2006**, *99*, 08N710.
16. Huang, Z.-M.; Zhang, Y. Z.; Kotaki, M.; Ramakrishna, S. *Compos. Sci. Technol.* **2003**, *63*, 2223.
17. Doshi, J.; Reneker, D. H. *J. Electrostat.* **1995**, *35*, 151.
18. Sun, Z.; Deitzel, J. M.; Knopf, J.; Chen, X.; Gillespie, J. W. *J. Appl. Polym. Sci.* **2012**, *125*, 2585.
19. Bognitzki, M.; Czado, W.; Frese, T.; Schaper, A.; Hellwig, M.; Steinhart, M.; Greiner, A.; Wendorff, J. H. *Adv. Mater.* **2001**, *13*, 70.
20. Megelski, S.; Stephens, J. S.; Chase, D. B.; Rabolt, J. F. *Macromolecules* **2002**, *35*, 8456.
21. Eda, G.; Liu, J.; Shivkumar, S. *Eur. Polym. J.* **2007**, *43*, 1154.
22. Mahaling, B.; Katti, D. S. *J. Mater. Sci.* **2014**, *49*, 4246.
23. Zong, X.; Kim, K.; Fang, D.; Ran, S.; Hsiao, B. S.; Chu, B. *Polymer* **2002**, *43*, 4403.
24. Shan, D.; Shi, Y.; Duan, S.; Wei, Y.; Cai, Q.; Yang, X. *Mater Sci Eng C* **2013**, *33*, 3498.
25. Takeda, M.; Kamagata, Y.; Ghiorse, W. C.; Hanada, S.; Koizumi, J.-I. *Int. J. Syst. Evol. Microbiol.* **2002**, *52*, 895.
26. Takeda, M.; Koizumi, J.-I.; Yabe, K.; Adachi, K. *J. Ferment. Bioeng.* **1998**, *85*, 375.
27. Barham, P. J.; Keller, A.; Otun, E. L.; Holmes, P. A. *J. Mater. Sci.* **1984**, *19*, 2781.
28. Bhatt, R.; Patel, K. C.; Trivedi, U. *J. Polym. Environ.* **2010**, *18*, 141.
29. Shivakumar, S.; Jagadish, S.; Zatakia, H.; Dutta, J. *Appl. Biochem. Biotechnol.* **2011**, *164*, 1225.
30. Kumagai, Y.; Doi, Y. *Polym. Degrad. Stab.* **1992**, *36*, 241.
31. Takeda, M.; Kitashima, K.; Adachi, K.; Hanaoka, Y.; Suzuki, I.; Koizumi, J.-I. *J. Biosci. Bioeng.* **2000**, *90*, 416.
32. Han, J.-S.; Son, Y.-J.; Chang, C.-S.; Kim, M.-N. *J Microbiol* **1998**, *36*, 67.
33. Wei, Y.; Zhang, X.; Song, Y.; Han, B.; Hu, X.; Wang, X.; Lin, Y.; Deng, X. *Biomed. Mater.* **2011**, *6*, 1.